



Planar Procrustes analysis of tooth shape

D.L. Robinson^{a,b,*}, P.G. Blackwell^b, E.C. Stillman^b, A.H. Brook^a

^a Department of Child Dental Health, School of Clinical Dentistry, University of Sheffield, Clarendon Crescent, Sheffield S10 2TA, UK

^b Department of Probability and Statistics, Hicks Building, University of Sheffield, Hounsfield Road, Sheffield S3 7RH, UK

Accepted 9 October 2000

Abstract

Accurate quantification of variation in tooth shape is important in studies of dental development, which typically have involved measuring distances between subjectively identified landmarks, key points of correspondence on teeth. An established statistical framework now exists for the analysis of shape when objects are represented as configurations of landmark coordinates; allowing work with the full geometry of objects, which is otherwise lost. This approach was introduced here to the study of tooth morphology, demonstrating how after optimally matching shapes to account for the unwanted effects of location, scale and rotation, most standard descriptive and inferential statistical techniques can be adapted and applied successfully. The techniques are illustrated using a sample of buccal-surface images of central incisors from patients with hypodontia; a significant difference is found in mean buccal-surface shape (Hotelling's two-sample T^2 -test; $P = 0.004$) when compared to a corresponding control group. Successful implementation of these methods depends on the accuracy and reliability with which the landmarks are collected; issues and problems to be addressed are discussed. © 2001 Elsevier Science Ltd. All rights reserved.

Keywords: Procrustes analysis; Tooth shape; Landmarks; Hypodontia

1. Introduction

Accurate measurement and analysis of tooth shape is important in studies of dental development. Identifying variation between individuals in population and family studies is valuable in understanding the genetic and environmental influences in conditions such as hypodontia and supernumeracy.

The study of tooth morphology, as with many other biological investigations of shape, has typically involved measuring selected distances, angles or ratios between subjectively identified 'landmarks'. Standard univariate and multivariate statistical techniques have then been employed to form inferences based on these

measurements (e.g. Fearn and Brook, 1993). Advances in digital imaging and scanning have aided the process of taking such measurements but also enable the locations of landmarks to be recorded as coordinates.

Over the last decade, numerous methodological approaches to the study of objects represented as landmark configurations have been consolidated into what Bookstein (1998) refers to as the 'morphometric synthesis', an established framework by which an investigation of shape should proceed. As these methods have become more well known, their use has become increasingly popular in a variety of disciplines, aided by the wider availability of computerised routines and software as well as the growth in accessible literature. Dryden and Mardia (1998) provide details of these methods with examples and have made available their own routines (<http://www.amsta.leeds.ac.uk/~iand/Shape-R/Shape-R.html>), which have been used and

* Corresponding author. Fax: +44-114-2717843.

E-mail address: d.l.robinson@sheffield.ac.uk (D.L. Robinson).

adapted for this paper. As the analysis is based on the configuration of landmarks, this allows one to work with the full geometry of objects, which is otherwise lost.

Here, we introduce these ideas to the study of tooth form, considering the common ‘planar’ case of data in two dimensions, where landmark locations have been recorded as (x, y) coordinates in the two-dimensional plane of a photographic image. For higher-dimensional data, the mathematical details are more complex, but the concepts involved remain the same (Dryden and Mardia, 1998, Ch. 5).

Using buccal images of central incisors from patients with hypodontia and a corresponding control group, we illustrate how it is possible to estimate mean shapes and investigate shape variability. We also demonstrate how conventional two-dimensional inferential techniques may be adapted to examine hypotheses about shape.

The final part of this paper discusses some of the issues and caveats associated with the implementation of planar Procrustes methods in comparing and describing variation in tooth shape.

2. Methods

2.1. Concepts

2.1.1. Landmarks

Landmarks are key points of correspondence, defined in the same way on each tooth of a given type and selected to be informative about particular characteristics of interest. Examples of buccal and occlusal tooth-surface landmarks are presented in Fig. 1. Landmarks may be ‘anatomical’ (as shown) or ‘mathematical’ (e.g. points of maximum curvature or diameter).

The locations of landmarks may be recorded as (x, y) coordinates on the two-dimensional plane of an image (Fig. 2). Conventionally, the x -axis of a two-dimensional image runs parallel to the bottom edge of the image window, with the perpendicular y -axis parallel to the left side of the image. Calibration typically involves placing a rule in the plane of the buccal or occlusal surface, before imaging, which is then used to specify the scale of the two axes.

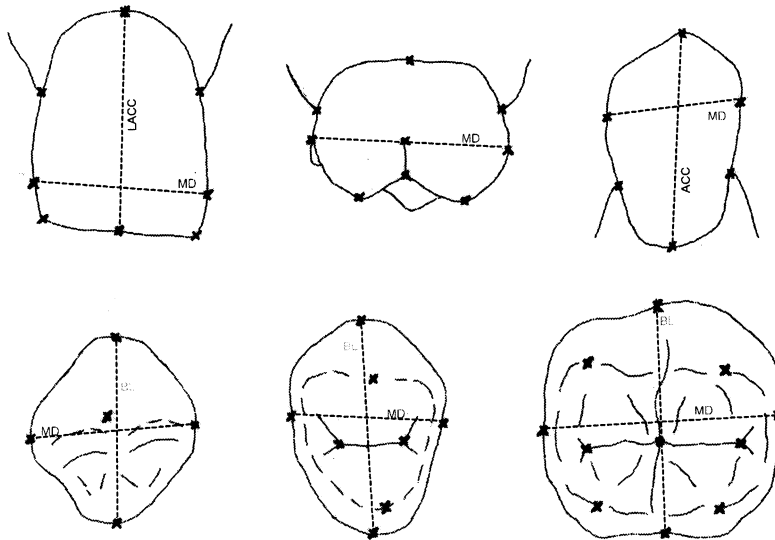


Fig. 1. Possible landmarks on various tooth types. Top row: buccal surfaces. (Left) Upper central incisor: Endpoints of mesiodistal (MD) width, endpoints of long axis of clinical crown (LACC), corners of incisal edge, endpoints of gingival margin. (Middle) Upper first molar: endpoints of mesiodistal width, mesial and distal cusp tips, endpoints of buccal groove, endpoints and middle of gingival margin. (Right) Lower canine: endpoints of mesiodistal width, endpoints of long axis of clinical crown (through cusp tip), endpoints of gingival margin. Bottom row: Occlusal surfaces. (Left) Lower canine: endpoints of mesiodistal (MD) width, endpoints of buccal–lingual width (BL), cusp tip. (Middle) Upper first premolar: endpoints of mesiodistal (MD) width, endpoints of buccal–lingual width (BL), cusp tips, fissure junctions (pits). (Right) Second molar: endpoints of mesiodistal (MD) width, endpoints of buccal–lingual width (BL), cusp tips, fissure junctions (pits).

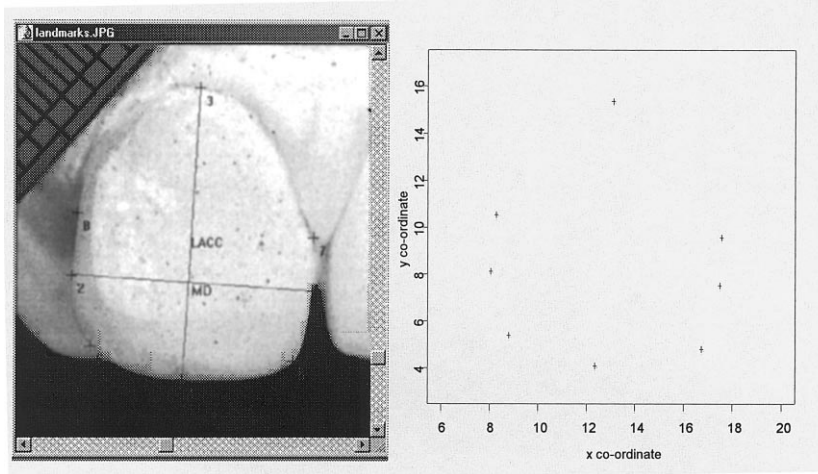


Fig. 2. Upper central incisor: (Left) image grabbed using Adobe PhotoShop and landmark coordinates recorded using Image Pro Plus; (Right) landmarks displayed as a two-dimensional plot in S-Plus.

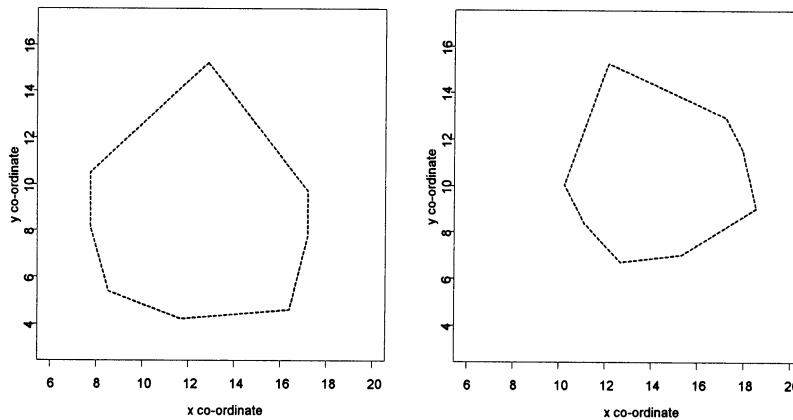


Fig. 3. Two landmark configurations with differences in coordinates (due to scale, rotation and location within the plane) but same shape.

2.1.2. Shape

Shape is defined by Dryden and Mardia (1998) as ‘all the geometrical information that remains when location, scale and rotational effects are filtered out from an object’. Similarly, Bookstein (1998) noted that: ‘In ordinary language, the shape of an object is described by words or quantities that do not vary when the object is moved, rotated, enlarged or reduced’. Because such transformations change the coordinates of sets of points without changing their shapes, distances between landmark locations obtained from different images are meaningless and so applying conventional two-dimensional statistical procedures directly to the landmark data would be inappropriate. One must therefore remove the unwanted ‘registration’ differences between configurations, i.e. coordinate differences due to loca-

tion, scale and rotation, so that meaningful measures of dissimilarity in shape may be defined.

Fig. 3 shows two incisor configurations that have exactly the same shape, but different sets of landmark coordinates, due to the registration of each tooth within its image.

2.1.3. Procrustes matching

Consider two configurations V and W , each consisting of k corresponding landmark coordinates, (v_{jx}, v_{jy}) in V and (w_{jx}, w_{jy}) in W for $j = 1, \dots, k$. A configuration may be rotated [about $(0,0)$] by θ radians anticlockwise, resized by factor β and each point shifted by ‘ a ’ units in the x -direction and ‘ b ’ units in the y -direction, to produce a new coordinate set of equivalent shape. For example, for W we can find W' with coordinates (w'_{jx}, w'_{jy}) given by:

$$(a + \beta(w_{jx} \cos \theta - w_{jy} \sin \theta), b + \beta(w_{jx} \sin \theta + w_{jy} \cos \theta)), j = 1, \dots, k$$

In order to compare the shapes of V and W and quantify how they differ, the configurations are matched as closely as possible using such transformations. If V and W have the same shape, it will be possible to match them exactly. In the notation above, W (say) is fitted to V , by finding the nearest equivalent configuration of W to V , i.e. we find the W' (with coordinates given by the equation above) which minimises

$$\sum_{j=1}^k ((w'_{jx} - v_{jx})^2 + (w'_{jy} - v_{jy})^2)$$

the sum of squared distances between the corresponding coordinates of W' and V ; (w'_{jx}, w'_{jy}) are then the 'fitted Procrustes coordinates' of W onto V .

In practice, the optimal match is achieved by carrying out the following series of operations: (1) centre; (2) resize; (3) rotate; (4) resize. That is, firstly, the configurations are translated [to (0, 0)] so that their centres are coincident. Secondly they are then resized so that each centroid size, i.e. sum of squared distances of landmarks to the configuration centre, is set equal to 1. One of the configurations is then rotated about (0, 0) until the sum of squared distances between corresponding landmarks is minimised. At this stage the minimised sum is known as the 'partial Procrustes' distance between the two shapes. It is then possible to reduce the sum of inter-landmark distances further, by resizing the rotated shape to obtain the 'full Procrustes' distance between configurations.

The procedure is illustrated in Fig. 4 where two landmark sets have been obtained from buccal images of two lower left canine teeth. In practice, particularly when there is only a small variation in shape, there is very little difference in an analysis based on 'full' or 'partial' Procrustes distances, as can be seen in the final part of Fig. 4.

2.2. Materials

Using a new image-analysis system (Brook et al., 1998), buccal images of 20 upper left central incisors were obtained from study casts of patients with moderate/severe hypodontia (three or more congenitally missing teeth). These patients' records are being investigated as part of a wider study of hypodontia for which ethics committee approval has been obtained.

Teeth partially obscured by crowding or with evidence of attrition were excluded. Six landmarks were identified on each image as defined in Fig. 1(a), with the exception of the mesiodistal endpoints, which in this population are difficult to locate.

A control sample of 20 such buccal images was also

obtained, following the same selection criteria, and the six corresponding landmarks to those identified on the hypodontia tooth images recorded.

2.3. Analysis of shape: descriptive

2.3.1. Procrustes estimate of mean shape

An estimate of mean shape $\hat{\mu}$, with coordinates $(\hat{\mu}_{jx}, \hat{\mu}_{jy})$, $j = 1, \dots, k$ may be obtained from a sample of landmark configurations W_i , $i = 1, \dots, n$, as the shape which has the least sum of Procrustes distances to each configuration in the sample. The Procrustes estimate of mean shape can be found by a variety of methods (e.g. Kent, 1994). Fitting each W_i to the estimated mean shape gives the 'full Procrustes fit', W_i^P , of each configuration, with fitted Procrustes coordinates $(w_{i,jx}^P, w_{i,jy}^P)$.

2.3.1.1. Example: mean buccal-surface shape of central incisors in patients with hypodontia. Fig. 5 shows the full Procrustes estimated mean buccal shape and full Procrustes fits of the hypodontia sample.

2.3.2. Investigating shape variability

A measure of the sample's variation in shape is the root mean square (rms) Procrustes distance, the square root of the mean-squared full Procrustes distance from each sample configuration to the full Procrustes mean.

The structure of shape variability in the sample may be investigated by principal components analysis (PCA), a method for summarising patterns of variation in a set of variables, here the coordinates of the Procrustes fits $(w_{i,jx}^P, w_{i,jy}^P)$, in terms of uncorrelated, linear combinations of these variables. Principal components are calculated so that they measure different aspects of shape variation. The first principal component, PC(1), represents the largest amount of variation in shape, PC(2) the second largest and so on, so that (hopefully) most of the variation in shape will be summarised by the first few components.

Principal component (r) is given by

$$\sum_{j=1}^k (\gamma_{rjx} w_{jx}^P + \gamma_{rjy} w_{jy}^P)$$

where the pairs of weights γ_{rjx} and γ_{rjy} describe directions of variation in each Procrustes coordinate about the mean shape [see, for example, Mardia et al. (1979) for a general description of PCA].

Visualisation involves displaying hypothetical configurations at different extremities of shape variation, in directions defined by the principal components. For PC(r), we can plot shapes with coordinates given by:

$$(\hat{\mu}_{jx} + c\sqrt{\lambda_r}\gamma_{rjx}, \hat{\mu}_{jy} + c\sqrt{\lambda_r}\gamma_{rjy})$$

where typically $-3 \leq c \leq 3$ and λ_r is the variance captured by $PC(r)$, so that configurations between -3 and $+3$ S.D. either side of the mean shape may be obtained.

2.3.2.1. *Example: shape variation of buccal surface of central incisors in patients with hypodontia.* We return to the Procrustes fit and mean shape obtained in the previous example. In Fig. 6, configurations at -3 , -2 ,

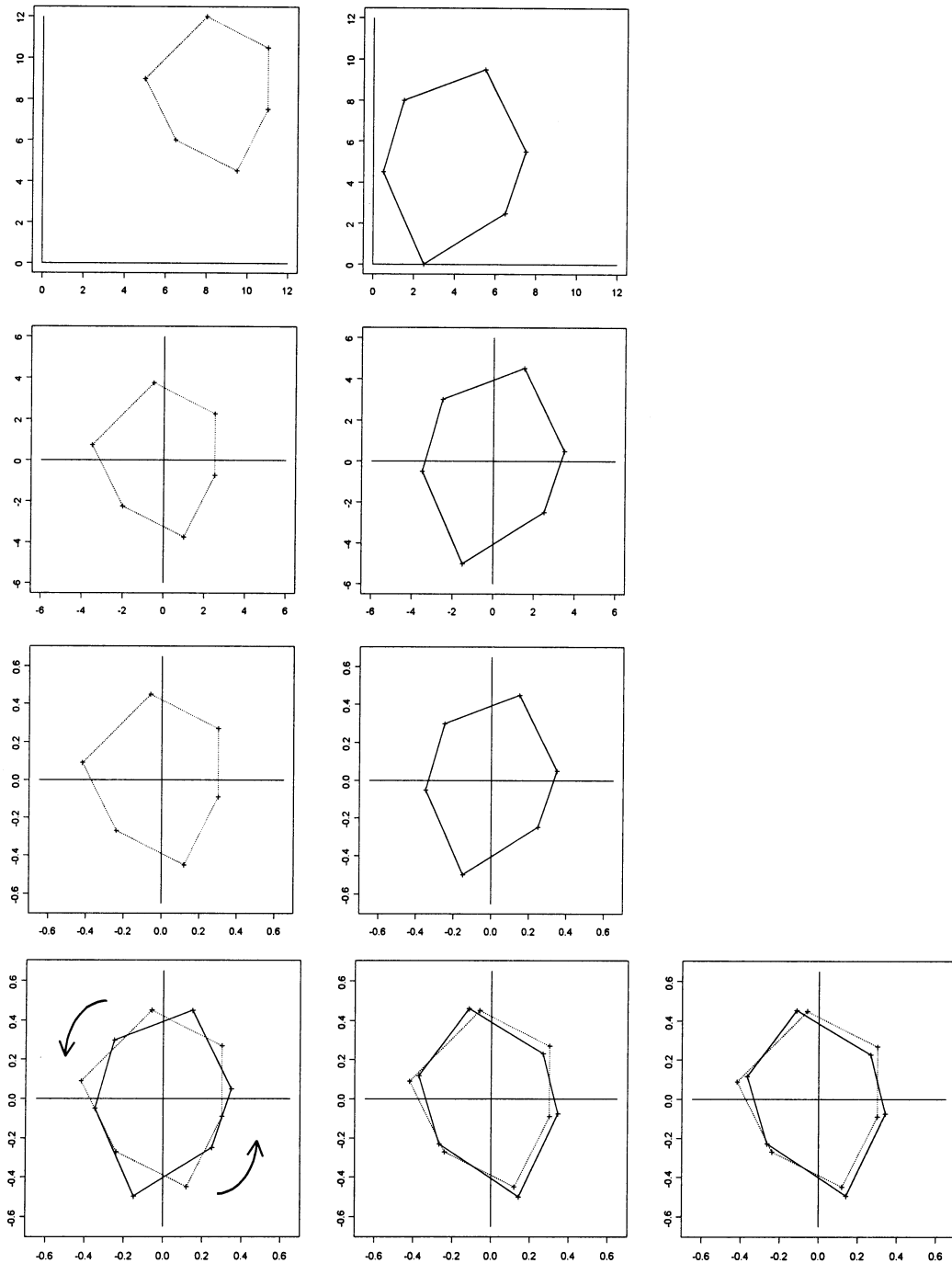


Fig. 4. Procrustes superimposition of two landmark configurations. (First row) Original recorded coordinates of each configuration on the image axes. (Second row) Centred and (third row) scaled version of each configuration. (Final row) Superimposition of the centred unit sized shapes before rotation (left), then the partial (middle) and full (right) Procrustes fit of configuration 2 (solid line) to configuration 1 (dotted line).

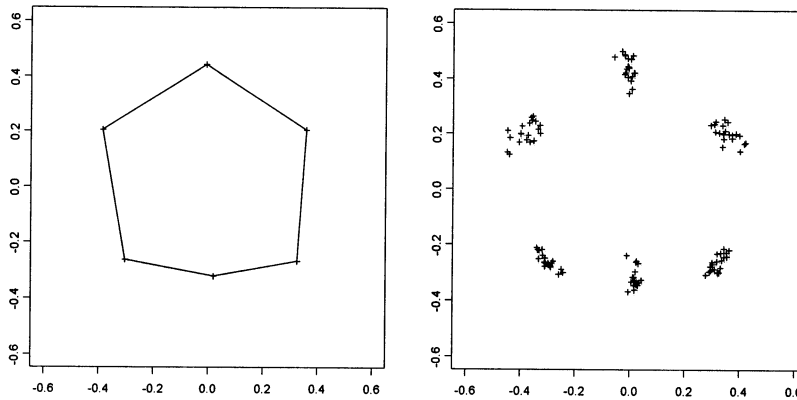


Fig. 5. (Left) full Procrustes mean shape and (right) full Procrustes fits of upper left hypodontia incisors, with gingival landmarks at the top, incisal landmarks at the bottom.

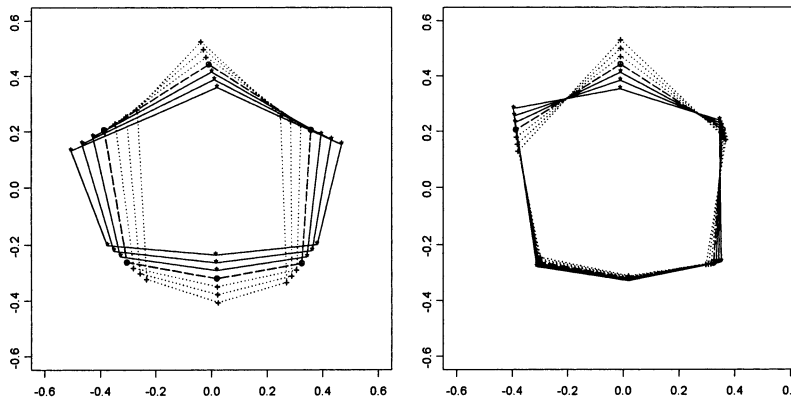


Fig. 6. (Left) Dotted lines: Shapes at -3 , -2 , -1 S.D. along the first PC of variation. Solid lines: Shapes at $+1$, $+2$, $+3$ S.D. along the first PC. Dashed lines: Procrustes mean shape. (Right) Dotted lines: Shapes at -3 , -2 , -1 S.D. along the second PC of variation. Solid lines: Shapes at $+1$, $+2$, $+3$ S.D. along the second PC. Dashed lines: Procrustes mean shape.

-1 and $+1$, $+2$, $+3$ S.D. either side of the mean shape are plotted in the directions of the first and second principal components of variation. PC(1) in Fig. 6 (left), accounts for 62% of the variation in shape in the sample and contrasts the length of the long axis of the clinical crown with the width of the tooth, particularly around the gingival margin. We see that relatively wider teeth are more 'tapered' in shape. PC(2) in Fig. 6 (right) accounts for just 15% of the variation in shape and reflects vertical variation in the central and distal gingival landmarks.

2.3.3. Deformation grids

One is frequently interested in comparing two shapes or sets of shapes. The Procrustes distance provides a numerical measure of dissimilarity but does not indicate where two configurations differ. One method for describing visually the difference between two configurations is to use a deformation grid.

Imagine one configuration drawn on a piece of squared graph paper, the other on plain paper. If we 'deform' the graph paper so that the corresponding landmarks of the two configurations can be placed directly over each other, the resulting deformed grid tells us where and how the configurations differ.

The deformation required to transform the space in which one configuration lies to match specific locations in the space of the other is estimated by a pair of functions called thin-plate splines. These define a mapping of all points in the first image to points in the second, constrained so that corresponding landmarks match exactly and the square grid 'bends' as little as possible, so the deformation is 'optimal'. We use a pair of splines for two-dimensional data, one for obtaining the new x -coordinates of the points, the other for obtaining the new y -coordinates. At each junction where the lines on the square-grid image cross, the corresponding position in the deformed image is calcu-

lated and the lines between the points re-drawn, so that corresponding landmarks are located in corresponding grid blocks (Dryden and Mardia, 1998, Ch. 10).

2.3.3.1. Example: comparison of hypodontia and control mean central incisor shape. In Fig. 7, a square grid superimposed onto the control mean shape is deformed to lie on the hypodontia mean shape. The result shows that the shapes differ in the position of the incisal corners, with central incisors being more tapered in shape in the hypodontia group.

2.4. Analysis of shape: inference

In data-sets with small variation in shape, as would be expected with any within-tooth type sample, one can carry out most of the usual multivariate statistical

techniques following Procrustes superimposition, such as testing for group differences in shape. Variation being small means that distances between the Procrustes fits and the estimated mean shape can be well approximated by distances in the 'tangent space' (Dryden and Mardia, 1998, Ch. 7).

The most useful multivariate techniques here are the one- and two-sample Hotelling's T^2 -tests for mean shape. The one-sample test can be used to obtain a confidence region for mean shape, this being the set of configurations for which a particular hypothesised shape is not rejected. For two independent samples, providing that the variation in shape is reasonably similar in each group (a formal comparison can be made using for example Box's M -test), Hotelling's T^2 -test can be used to test the null hypothesis of no difference in mean shape between two groups.

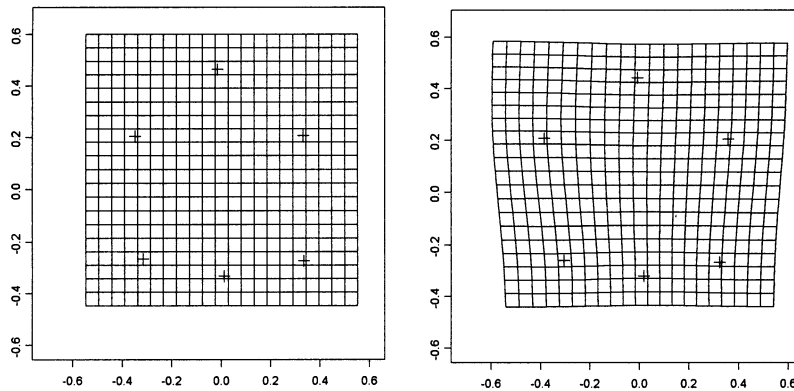


Fig. 7. (Left) Square grid superimposed onto the control mean central incisor shape. (Right) Square grid deformed to lie on the mean shape of the hypodontia group.

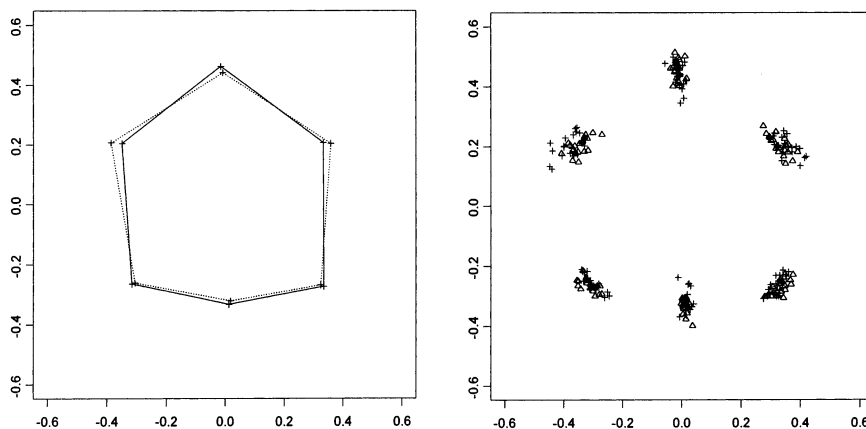


Fig. 8. (Left) Superimposed Procrustes mean shapes of control (solid) and hypodontia (dashed) upper left central incisors. (Right) Procrustes fits using a pooled sample (Δ , control; +, hypodontia). Gingival landmarks at top of plots.

2.4.1. Example: comparison of central incisor buccal-surface shape; hypodontia versus control group

We consider the upper left central incisors from the hypodontia and control samples. Fig. 8 (left) shows the full Procrustes mean from the control sample matched to the estimated mean shape of the hypodontia sample. Fig. 8 (right) shows the scatter of Procrustes fits for each group around the pooled mean shape. The test statistic follows an F -distribution and the observed value gives a P -value of 0.004, providing strong evidence of a difference between the hypodontia and control incisor shapes. As suggested by the exploratory analysis (Fig. 7), the mean shapes differ in the position of the incisal corners, hypodontia central incisors being more tapered in shape.

3. Discussion

As the Procrustes approach becomes more established, its application to various biological disciplines is becoming increasingly widespread. Examples of studies making use of these methods can be found from many fields, from zoology to medicine (e.g. Kingenburt and Bookstein, 1998).

This paper introduces a formal definition of shape and demonstrates its application in the study of tooth morphology. In particular, in a study of patients with hypodontia, this accurate description of central incisor morphology allowed differentiation between affected individuals and controls.

As with any other method of analysis, successful implementation depends on the accuracy and reliability with which data (here the landmarks) are collected. Systematic errors will result in false representations of shape. Identification inconsistencies in the positions of landmarks will carry through into the inferential procedures, inflating residual variance and so diluting 'real' differences between individuals.

In order to provide an introduction to Procrustes methods we have considered the case of 'planar' data, typically obtained when three-dimensional structures are reduced to two dimensions by digital imaging. Of course, the buccal surface of a central incisor is not a perfectly flat surface and the two-dimensional representation will be a distortion of the three-dimensional reality, especially at the edges. However, for the surfaces in question this distortion is expected to be small and all methods operating on two-dimensional images will be subject to the same difficulties.

A further potential source of error is in the subjective orientation of the tooth surface when its two-dimensional image is captured. Our experience shows that with standardised instructions, inter-operator inconsistencies of this type are small for the surfaces considered here. For some imaging systems an additional error

arises from perspective effects if the camera is placed close to the surface (Arnqvist and Martensson, 1998). For the Sheffield system, the distance of the camera from the tooth is sufficiently large for this to be inconsequential.

If one is genuinely interested in the tooth as a three-dimensional object then any purely two-dimensional method is inadequate. However, the approach described here can be applied to three-dimensional landmarks when such data are available. Technical details are given in Dryden and Mardia (1998) (Ch. 5).

Once the tooth image has been captured, certain landmarks, such as those at the corners of the incisal edge and the mesiodistal width, can then be more difficult to identify than others, such as cusp tips or fissure junctions, which has implications in an analysis where each landmark carries equal 'importance'.

Other 'nuisance' variation results from the irregularity of the gingival margin on different individuals. Teeth may have the same shape but differences in their landmark coordinates due to the relative position of the gum around each tooth. Similar problems will result from attrition, causing landmarks to be difficult to locate and inflating variation in these regions. Crowding may mean that certain landmarks are impossible to identify.

Future work is intended to quantify and investigate the importance of these problems and to produce a coherent methodology for the analysis of tooth shape. A principal aim is to develop techniques for investigating the dependence of shape on explanatory variables. For example, one might often be interested in the interdependence of tooth size and shape, or seek genetic explanations for differences between groups.

Acknowledgements

The hypodontia and control buccal-surface images were taken by Mohammad Al-Sharood, postgraduate student, Department of Child Dental Health, School of Clinical Dentistry, University of Sheffield, Sheffield, UK.

Appendix A

A configuration 'A', of k landmark coordinates of the form (a_{jx}, a_{jy}) , $j = 1, \dots, k$, has centre (centroid) coordinates given by

$$(a_{cx}, a_{cy}) = \left(\frac{1}{k} \sum_{j=1}^k a_{jx}, \frac{1}{k} \sum_{j=1}^k a_{jy} \right)$$

and 'centroid size' given by

$$S = \sqrt{\sum_{j=1}^k ((a'_{jx} - a_{cx})^2 + (a'_{jy} - a_{cy})^2)}$$

The new coordinates (a'_{jx}, a'_{jy}) , resulting from transforming A so that the centre is at the origin and the configuration is of unit size, are given by:

$$\left(\frac{1}{S}(a_{jx} - a_{cx}), \frac{1}{S}(a_{jy} - a_{cy}) \right), j = 1, \dots, k$$

If two configurations V and W have previously been 'centred' and scaled to unit centroid size, a and b in the equations for transforming W will both be zero. The optimal rotation θ and scale β , to give the full Procrustes fit of W to V are then:

$$\theta = \tan^{-1} \left(\frac{\sum_{j=1}^k (w_{jx}v_{jy} - w_{jy}v_{jx})}{\sum_{j=1}^k (w_{jx}v_{jx} + w_{jy}v_{jy})} \right)$$

and

$$\beta = \sqrt{\left(\sum_{j=1}^k (w_{jx}v_{jx} - w_{jy}v_{jy}) \right)^2 + \left(\sum_{j=1}^k (w_{jx}v_{jy} - w_{jy}v_{jx}) \right)^2}$$

For a proof and further details, see Dryden and Mardia (1998) (Ch. 3).

References

- Arnqvist, G., Martensson, T., 1998. Measurement error in geometric morphometrics: Empirical strategies to assess and reduce its impact on measures of shape. In: Kingenburgh, C.P., Bookstein, F.L. (Eds.), *Acta Zool. Sci. Hung.* 44(1–2) 73–96.
- Bookstein, F.L., 1998. A hundred years of morphometrics. In: Kingenburgh, C.P., Bookstein, F.L. (Eds.), *Acta Zool. Sci. Hung.* 44(1–2) 7–59.
- Brook, A.H., Smith, R.N., Elcock, C., Al-Sharood, M.H., Shah, A., Karmo, M., 1998. The measurement of tooth morphology: Development and validation of a new image analysis system. In: Mayhall, J., Heikkman, T. (Eds.), *Dental Morphology*. Oulu University Press, Finland, pp. 380–388.
- Dryden, I.L., Mardia, K.V., 1998. *Statistical Shape Analysis*. Wiley, New York.
- Fearne, J.M., Brook, A.H., 1993. Small primary tooth crown size in low birthweight children. *Early Hum. Dev.* 33, 81–90.
- Kent, J.T., 1994. The complex Bingham distribution and shape analysis. *J. R. Stat. Soc. Ser. B* 56, 285–299.
- Kingenburgh, C.P., Bookstein, F.L. (Eds.), 1998. *Acta Zool. Sci. Hung.* 44(1–2), 1–194.
- Mardia, K.V., Kent, J.T., Bibby, J.M., 1979. *Multivariate Analysis*. Academic Press, London.